

# Hexagonal spin structure of $A$ -phase in MnSi: densely packed skyrmion quasiparticles or two-dimensionally modulated spin superlattice?

*S. V. Grigoriev<sup>+\*1)</sup>, N. M. Potapova<sup>+</sup>, E. V. Moskvina<sup>+\*</sup>, V. A. Dyadkin<sup>+\*</sup>, Ch. Dewhurst<sup>o</sup>, S. V. Maleyev<sup>+</sup>*

<sup>+</sup>*Konstantinov Petersburg Nuclear Physics Institute, 188300 Gatchina, Russia*

<sup>\*</sup>*S.-Petersburg State University, 198504 S.-Petersburg, Russia*

<sup>×</sup>*Swiss-Norwegian Beamlines at the European Synchrotron Radiation Facility, 38000 Grenoble, France*

<sup>o</sup>*Institute Laue-Langevin, F-38042 Grenoble Cedex 9, France*

Submitted 16 June 2014

Resubmitted 7 July 2014

We have studied in detail the  $A$ -phase region in the field-temperature ( $H$ – $T$ ) phase diagram of the cubic helimagnet MnSi using small angle neutron diffraction. The  $A$ -phase revealed itself as a two-dimensional hexagonal pattern of Bragg spots with  $\mathbf{k}_{h(1,2,3)} \perp \mathbf{H}$ . The directions and value of wave-vectors  $\mathbf{k}_{h(1,2,3)}$  are well preserved over the whole crystal of the size of 100 mm<sup>3</sup>, but in the small room of the ( $H$ – $T$ ) phase diagram just below  $T_c = 29$  K. The droplets of the orientationally disordered, presumably hexagonal, spin structure with  $\mathbf{k}_h \perp \mathbf{H}$  are observed in the wide range beyond the  $A$ -phase boundaries in the field range from  $B_{T1} \approx 0.1$  T to  $B_{T2} \approx 0.25$  T at temperatures down to 15 K. No melting of these droplets into individual randomly located skyrmions is observed for all temperatures and magnetic fields. The wavevector of two dimensional modulations  $k_h$  is equal to the wavevector of the cone phase  $k_c$ . We conclude that observable is a two dimensionally modulated hexagonal spin superlattice built on the same competition of interactions (ferromagnetic exchange and Dzyaloshinsky–Moriya interaction) similar to a case of one-dimensionally modulated simple spin spiral.

DOI: 10.7868/S0370274X14150132

The long-period spin spiral observed in MnSi with use of small angle neutron scattering was considered for a long time as one more curious example of the natural complexity of the magnetic structures [1]. The theoretical consideration had approved that this spiral structure is induced by the antisymmetric Dzyaloshinskii–Moriya (DM) exchange interaction competing to the ferromagnetic exchange interaction (FEI) [2, 3]. The DM interaction in such systems appears as a result of the noncentrosymmetric cubic crystal structure of the B20 type (space group P2<sub>1</sub>3) [4]. Additionally, the spin spiral structure becomes homochiral predetermined by the handedness of a given crystal [5, 6]. The above-mentioned facts are well established and repeatedly proven in many neutron scattering experiments.

At present several concepts and many experimental studies are focused on a small pocket in the  $H$ – $T$  phase diagram close to  $T_c$  ( $A$ -phase). Though the existence of such a pocket had been first reported in MnSi as long as in 1976 [7], at present it is found in the vast variety of

the magnetic materials with B20-type of structure [8–19]. The nature of the  $A$ -phase was revealed in the neutron scattering experiments as a static magnetic modulation propagating perpendicularly to the applied field in MnSi [10, 11] and in Fe<sub>*x*</sub>Co<sub>1–*x*</sub>Si [8, 12, 13]. Later on  $A$ -phase was identified as a hexagonal magnetic lattice with  $\mathbf{k}_{h(1,2,3)} \perp \mathbf{H}$  in MnSi [14] and in various compounds of the transition metal monosilicides Mn/FeSi, Mn/CoSi, Fe/CoSi [15–17] and in FeGe [18, 19]. Moreover, the  $A$ -phase structure demonstrates an exceptionally well-defined long-range order and the higher order scattering is an order of magnitude smaller than the parasitic double scattering effects [20].

The authors of [14] proposed a Landau–Ginsburg mean-field model describing single domain multi(three)- $\mathbf{k}$  structure, denoted as a skyrmion lattice. The authors argued that although a topologically nontrivial entity, i.e. skyrmion, is less energetically favorable as compared to the simple spiral structure in zero field, but it is possible to show that Gaussian thermal fluctuations in the vicinity of  $T_c$  stabilizes the triple- $\mathbf{k}$  structure under applied field.

<sup>1)</sup>grigor@pnpi.spb.ru

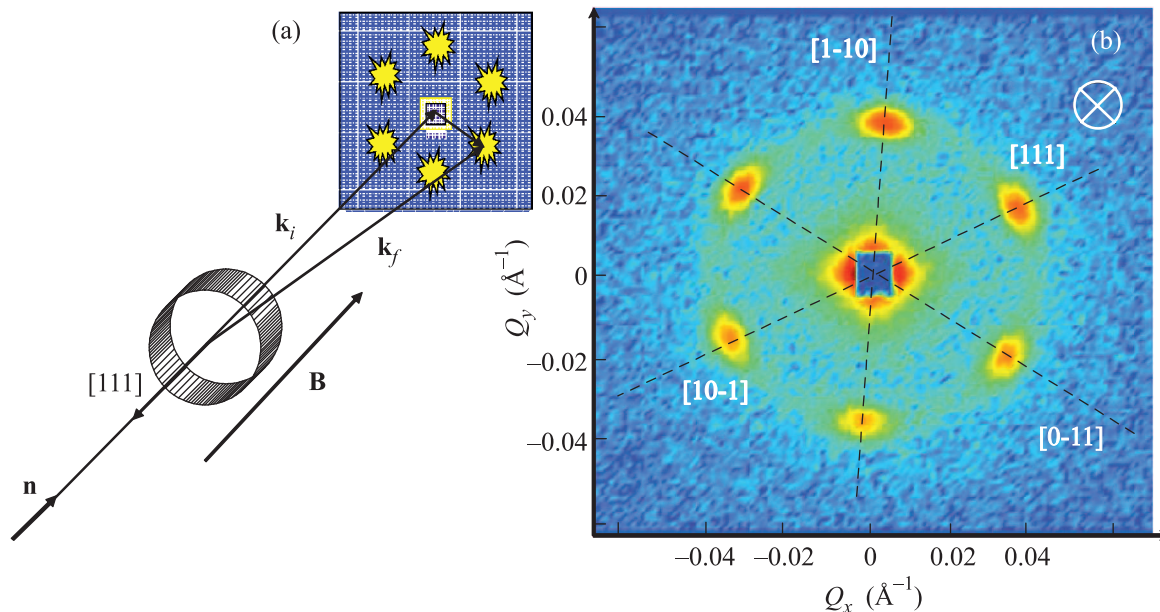


Fig. 1. (Color online) (a) – The outline of the scattering experiment with the field  $\mathbf{H}$  parallel to the neutron beam. (b) – The scattering map for the field-to-crystal orientation ( $\mathbf{B} \parallel [111]$ ) at  $T = 27.5$  K and  $B_{\text{int}} = 0.17$  T

The hexagonal skyrmion lattice was also observed in real space of the thin films in Fe/CoSi [21], FeGe [22] and MnSi [23] using Lorentz TEM. It was shown that the two-dimensional lattice is very stable over the large temperature and magnetic field ranges for the film thickness smaller than the spiral pitch  $d_s$ . It was also shown that the lattice constant of the skyrmion crystal  $d_{sk}$  is equal to the pitch  $d_s$ . It is worthwhile to note that isolated skyrmions or defects were really observed in the thin films  $\text{Fe}_{0.5}\text{Co}_{0.5}\text{Si}$  on the border between *A*-phase and the ferromagnetic state. However, the existence of such objects in thin films is not necessarily guaranteed their appearance in the bulk samples.

A theoretical concept of skyrmions in MnSi appearing above  $T_c$  and in the *A*-phase was introduced by Rößler et al. [24]. Building blocks of the skyrmion matter are the chiral flux-lines. This skyrmionic lattice is a two-dimensionally modulated spin texture. It competes with the common one-dimensional modulation (spin helix). Contrary to the spin helix, skyrmion lattice is characterized by a strong variation of the cell sizes and transformation of its structure near the cell boundaries. According to [25] the skyrmion-skyrmion interactions depends on the skyrmion density and temperature: it is repulsive in a broad temperature range, while it becomes oscillatory with alternating sign at high temperature (near  $T_c$ ). Close to  $T_c$  skyrmions are energetically confined, because pairs or cluster of skyrmions can achieve lower energies than the same number of the free skyrmions. Thus, skyrmions form the hexagonal lattice

with the lattice period equal to 1.27 of the spiral pitch  $d_s$  [25]. It is obvious in this concept that the periodicity of the skyrmion lattice is temperature and magnetic field dependent since it is fixed by the inter-skyrmion coupling but not correlated to the strength of the DM interaction.

At present there are two major concepts, which describe differently the origin of the *A*-phase in MnSi and relative compounds. One concept insists on the real skyrmionic character of the *A*-phase, where skyrmions as quasi-particles can build clusters of the hexagonal structure with the periodicity not related to the spiral pitch [24, 25]. Another concept claims the *A*-phase as an extremely stable long range order (skyrmion lattice), which skyrmionic nature is determined by the topologically protected knots and windings in the magnetic structure [14]. The existence of this topological winding is proven by the Hall effect measurements [26]. One may think that these concepts describes one and the same skyrmion lattice, which is not the case. The former one insists on the quasi-particle properties of the skyrmions, while the latter one describes the skyrmion lattice based on the DM interaction but it is focused on the skyrmion-like topology of its unit cell.

In this Letter we have revisited the cubic helimagnet MnSi to address the question of the origin of *A*-phase. The search for an individual skyrmion or their clusters at boundaries of the *A*-phase and well beyond required the use of a powerful (in sense of its intensity) SANS instrument. The small angle neutron diffraction experi-

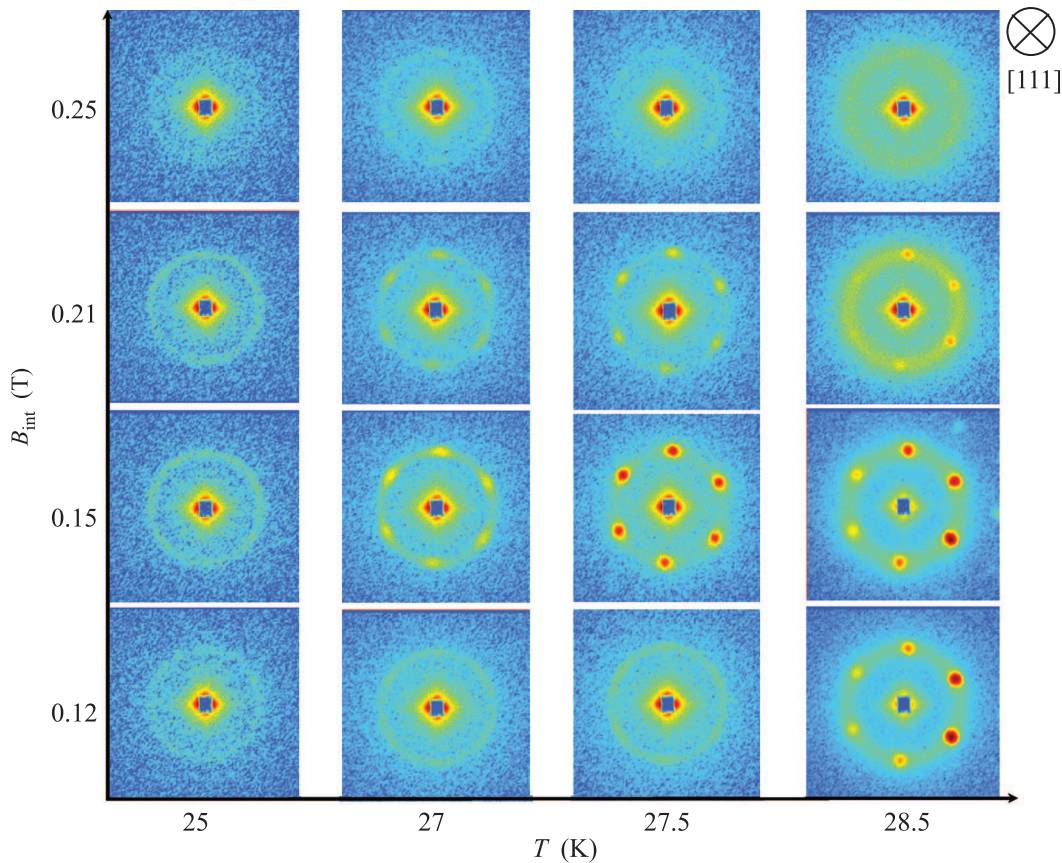


Fig. 2. (Color online) Scattering intensity maps plotted on the magnetic field–temperature ( $B$ – $T$ ) phase diagram for the field-to-crystal orientation  $\mathbf{B} \parallel [111]$

ments were carried out at the large dynamic range SANS facility D22 at the ILL (Grenoble, France). We used the same experimental geometry as was described in [14] when the magnetic field was applied along the neutron beam (Fig. 1a). The single crystal of MnSi used in [11] was chosen for the study. It was a disc with a thickness of 1.5 mm and a diameter of 15 mm. The [111] axis of the B20 structure was normal to the disc's plane and oriented along the field axis. The mosaic of the crystal does not exceed  $0.25^\circ$ . Hunting for the individual skyrmions we performed detailed field scans in the wide temperature range between 2 and 29 K after zero field cooling (ZFC).

A typical example of the scattering pattern is shown in Fig. 1b. The hexagonal pattern of the Bragg peaks are observed for at  $T = 27.5$  K and  $B_{\text{int}} = 0.17$  T [27]. The reflections lay on the three  $(\bar{1}\bar{1}0)$  axes in the [111] plane in accord with the previous studies. The orientation of the hexagonal pattern within  $A$ -phase is very stable and does not change with temperature or magnetic field. We conclude that the observed structure is a two-dimensionally modulated spin superlattice

(skyrmion lattice) with  $k_h = 0.38 \text{ nm}^{-1}$ , which coincides with the wavevector of the spiral at zero field. Another feature of the pattern is that the higher order reflections of this structure are strongly suppressed. All visible spots appearing with  $Q > k_h$  are fake coming from the double scattering process. This suppression of high order harmonics must be related to the exotic shape of these two-dimensional modulations being close to the harmonic laws. The strong suppression of the higher-order reflections was recently discussed in [20].

The evolution of the hexagonal patterns with temperature and the magnetic field can be followed in Fig. 2. The temperature changes are shown in the images along the horizontal line while the magnetic field scans correspond to the images along the vertical line in Fig. 2. The hexagonal well resolved scattering pattern with  $\mathbf{Q} \perp \mathbf{H}$  is observed at  $T$  close to  $T_c$  (on the right side of Fig. 2, i.e. above 27 K) in the intermediate field range  $0.12 < B_{\text{int}} < 0.21$  T. Its intensity changes with the field for the 2–3 orders of magnitude. As the neutron beam illuminates the whole MnSi crystal of the size of  $100 \text{ mm}^3$ , the obtained image demonstrates the coherency in the

structural orientation spreading over the crystal. The hexagon pattern transforms into the ring on the left side of Fig. 2, i.e. at  $T = 25$  K. The length of the wavevector  $k_h$  corresponding to the ring is well defined, while the orientational order of the (presumably hexagonal) pattern is completely lost. We associate this ring with the randomly oriented droplets of the A-phase at low temperatures.

For quantitative analysis the intensity maps were azimuthally averaged and the radial profiles (the  $Q$ -dependence of the scattering intensity) is given in Fig. 3. Two contributions (A-phase and critical fluctuations)

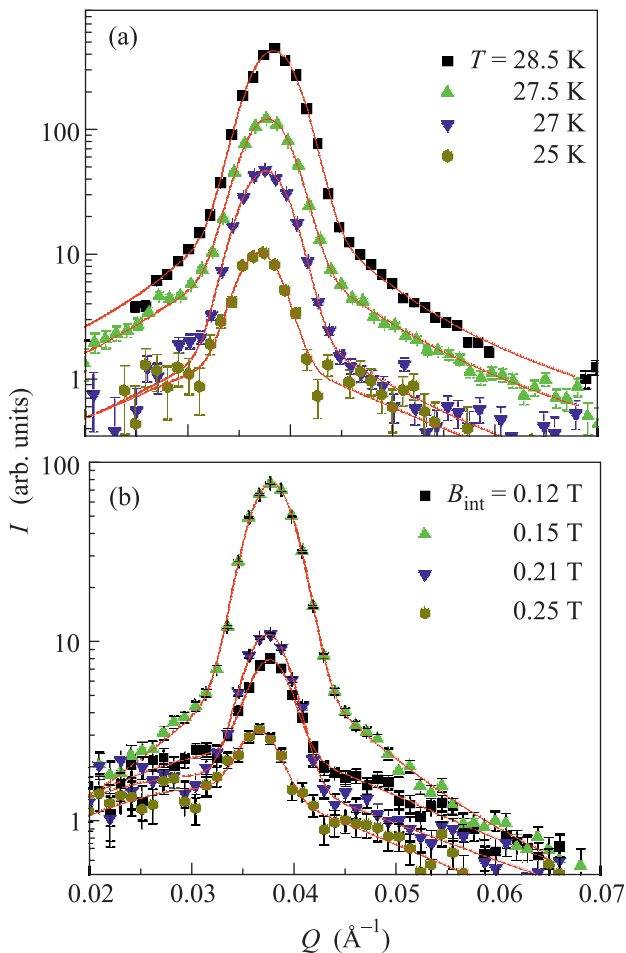


Fig. 3. (Color online)  $Q$ -dependence of the azimuthally averaged scattering intensity for the orientation ( $\mathbf{H} \parallel [111]$ ):  $B_{\text{int}} = 0.17$  T and  $T = 28.5, 27.5, 27.0, 25$  K (a);  $T = 27.5$  K and  $B_{\text{int}} = 0.12, 0.15, 0.21, 0.25$  T (b)

can be clearly distinguished in the  $Q$ -dependence of the scattering intensity. The scattering curve  $I(Q)$  can be well described by the sum of the Gaussian (A-phase structure) and Lorentzian (critical fluctuations) at  $T = 28.5$  and  $T = 27.5$  K. The Lorentz-shaped contri-

bution (critical fluctuations) diminishes at lower temperatures  $T = 27$  K and  $25$  K. Here we emphasize only that the contribution of the critical fluctuations can be clearly separated from the scattering from the A-phase structure but the interplay and interconnection of two contributions will be a subject of a different paper.

The A-phase is characterized by the Gaussian with the center  $k_h \approx 0.038 \text{ \AA}^{-1}$ . The peak width is limited by instrument resolution ( $0.004 \text{ \AA}^{-1}$ ) for all temperatures and magnetic fields. One can estimate from this uncertainty that this structure is coherent over more than 10 lattice periods even for these droplets well beyond the A-phase. We emphasize that no melting of the superlattice to the individual skyrmions or clusters was observed. We also suppose on the basis of the previous measurements [10, 11] that the droplets of the structure with  $\mathbf{k}_h \perp \mathbf{H}$  are surrounded by the cone phase with  $\mathbf{k}_c \parallel \mathbf{H}$ .

The integral intensity of the Gaussian is plotted in Fig. 4 as a function of the internal field  $B_{\text{int}}$  at different

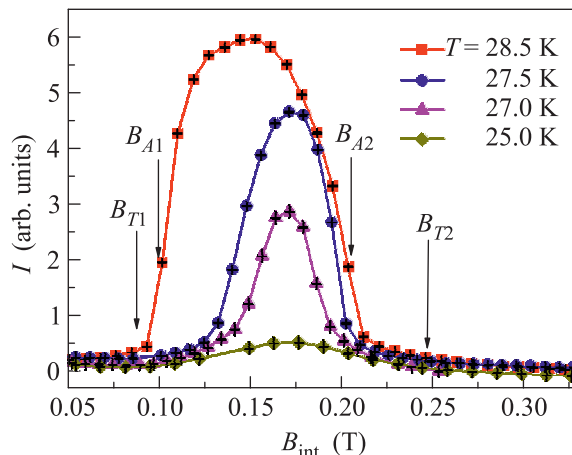


Fig. 4. (Color online) Integral intensity of the Bragg peak versus magnetic field  $B_{\text{int}}$  at different temperatures after zero field cooling.  $B_{T1}$  and  $B_{T2}$  are the critical fields where the droplets of the A-phase appear/disappear, respectively.  $B_{A1}$  and  $B_{A2}$  are the critical fields where the oriented A-phase structure appear/disappear, respectively

temperatures. We have taken into account the demagnetizing field because it is not negligible accounting for the shape of the disc-like sample [27]. The experimental curves exhibit a well defined maxima at the intermediate field range and vanishing intensity elsewhere. We indicate the boundaries of a distinct hexagonal pattern – the A-phase boundaries – as  $[B_{A1}, B_{A2}]$ . On both sides of this range we observe the regions of smooth increase/decrease of intensity ascribed to the droplets of the A-phase. These droplets appear/disappear at



the lower/upper critical fields  $B_{T1}, B_{T2}$ , respectively. The values of  $B_{T1}, B_{T2}, B_{A1}, B_{A2}$  are indicated by the arrows in Fig. 4 taking as an example the curve at  $T = 28.5$  K.

It is possible with these data to map the  $B$ - $T$  phase diagram based solely on the neutron diffraction experiment (Fig. 5). We have detected the single pocket of the

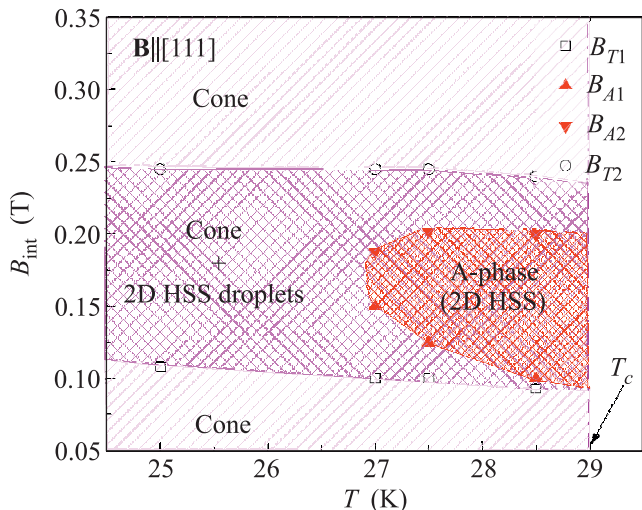


Fig. 5. (Color online) The  $B$ - $T$  phase diagram close to the  $A$ -phase of MnSi for the field  $\mathbf{B}$  applied along the  $[111]$  axis

two-dimensional hexagonal spin structure (“skyrmion lattice”) with  $\mathbf{k}_h \perp \mathbf{H}$ , appearing in a narrow range of the fields close to  $T_c$  (the  $A$ -phase). This pocket is limited by the lower boundary  $B_{A1}$  with its monotonic decrease with temperature whereas the upper boundary,  $B_{A2}$  does not depend on temperature. The “skyrmion lattice” with the orientational order ( $\mathbf{k}_h$ ) well preserved over the whole crystal dominates in this region over the conical phase.

The  $A$ -phase structure exists also within the field corridor  $[B_{T1}, B_{T2}]$  and down to low temperatures as small droplets dissolved in the cone phase. Although amount of these droplets decreases with lowering temperature, no indication of melting of these droplets into individual randomly located skyrmions was observed. The values of  $B_{T1}$  and  $B_{T2}$  are temperature independent. This observation of the temperature independent field corridor, where the droplets of the  $A$ -phase can appear, requires a new theoretical effort to comprehend the nature and origin of the  $A$ -phase. The  $A$ -phase at the low temperatures was reported in the  $\text{Fe}_{1-x}\text{Co}_x\text{Si}$  compounds [17] and in the MnSi doped by Ge [28] as the metastable state after the field cooling procedure. This metastable behaviour is clearly related to the presence of disorder, which is not the case for the present study of the pure MnSi crystal. Particularly, the droplets of the

$A$ -phase are observed at low temperature in the field scans after the zero-field cooling procedure. It is worthy to note that these droplets are not detected below 5 K.

It is well established in accord with the earlier observations [10, 11] that the wave-vector of the hexagonal structure  $k_h$  (in the  $A$ -phase) is equal to the wavevector of the spiral structure  $k_s$  with accuracy of 2% ( $k_s \approx 0.38 \text{ nm}^{-1}$  at  $T \sim T_c$ ). This observation is also in agreement with what is found in the thin films [21–23]. This experimental fact taken together with the absence of scattering from the individual skyrmions rule out the theory insisting on the real skyrmionic character of the  $A$ -phase, where skyrmionic quasi-particles might build clusters of the hexagonal  $A$ -phase structure [24, 25]. We believe that the observed structure is a two-dimensionally modulated hexagonal spin superlattice, which is built by the same competition of interactions as the one-dimensional superlattice (simple spin spiral) with  $k_h = k_s \approx D/J$ , where  $D$  is the Dzyaloshinskii constant,  $J$  is the exchange constant.

This structure should be viewed not as a collection of quasiparticles, but as a superposition of waves, namely three helices whose wavevectors form an equilateral triangle. Interesting also to note that accounting for the three-fold symmetry of the hexagon  $A$ -phase patterns the distance between the neighboring knots in the real-space superlattice should be equal to  $(2/\sqrt{3})d_s$ , where  $d_s$  is the periodicity of the one dimensional spiral structure. This fact implies that not the topologically protected knots determine the  $A$ -phase lattice but rather the energy landscape of the B20 crystals ( $D$  and  $J$ ) together with the magnetic field  $\mathbf{B}$  dictate the appearance of these knots. The former ( $D$  and  $J$ ) determine the distance between the knots and the latter  $\mathbf{B}$  orients the plane of the two-dimensional modulations. Finally, the  $A$ -phase crystal rather mimics the skyrmion lattice being in reality one more curious example of the complex magnetic structures. The complexity of the structure is emphasized by the two dimensional nature of its modulations which differentiates it from the one-dimensional modulations of a simple spiral or conical state. Probably, recently developed microscopic theory [29, 30] and/or calculations of spin wave dynamics of a skyrmion crystal treating it as a spin-density wave [31] may shed a new light to the origin of the  $A$ -phase and its structure.

Authors thank for partial support the Russian Foundation of Basic Research (Grants # 10-02-01205-a and 13-02-00160-a, 14-22-01073).

1. Y. Ishikawa, K. Tajima, D. Bloch, and M. Roth, Solid State Commun. **19**, 525 (1976).
2. P. Bak and M. H. Jensen, J. Phys. C **13**, L881 (1980).

3. I. E. Dzyaloshinskii, ZhETF **46**, 1420 (1964) [Sov. Phys. JETP **19**, 960 (1964)].
4. Historically the Dzyaloshinsky–Moria interaction was first introduced to explain the phenomenon of weak ferromagnetism in centrosymmetric crystals. Generally the presence/absence of DM interaction is associated with the local symmetry of the interatomic bonds and it leads to a spiral twist of the magnetic structure in magnets without inversion center.
5. M. Tanaka, H. Takayoshi, M. Ishida, and Ya. Endoh, J. Phys. Soc. J. **54**, 2970 (1985).
6. M. Ishida, Ya. Endoh, S. Mitsuda, Yo. Ishikawa, and M. Tanaka, J. Phys. Soc. J. **54**, 2975 (1985).
7. S. Kusaka, K. Yamamoto, T. Komatsubara, and Y. Ishikawa, Solid State Commun. **20**, 925 (1976).
8. K. Ishimoto, H. Yamaguchi, Y. Yamaguchi, J. Suzuki, M. Arai, M. Furusaka, and Y. Endoh, J. Magn. Magn. Mat. **90&91**, 163 (1990).
9. K. Ishimoto, Y. Yamaguchi, J. Suzuki, M. Arai, M. Furusaka, and Y. Endoh, Physica B **213&214**, 381 (1995).
10. B. Lebech, P. Harris, J. Skov Pedersen, K. Mortensen, C.I. Gregory, N.R. Bernhoeft, M. Jermy, and S. A. Brown, J. Magn. Magn. Mater. **140**, 119 (1995).
11. S. V. Grigoriev, S. V. Maleyev, A. I. Okorokov, Yu. O. Chetverikov, and H. Eckerlebe, Phys. Rev. B **73**, 224440 (2006).
12. S. V. Grigoriev, S. V. Maleyev, V. A. Dyadkin, D. Menzel, J. Schoenes, and H. Eckerlebe, Phys. Rev. B **76**, 092407 (2007).
13. S. V. Grigoriev, V. A. Dyadkin, Yu. O. Chetverikov, D. Menzel, J. Schoenes, A. I. Okorokov, H. Eckerlebe, and S. V. Maleyev, Phys. Rev. B **76** 224424 (2007).
14. S. Mühlbauer, B. Binz, F. Jonietz, C. Pfleiderer, A. Rosch, A. Neubauer, R. Georgii, and P. Böni, Science **323**, 915 (2009).
15. C. Pfleiderer, T. Adams, A. Bauer, W. Biberacher, B. Binz, F. Birkelbach, P. Böni, C. Franz, R. Georgii, M. Janoschek, F. Jonietz, T. Keller, R. Ritz, S. Mühlbauer, W. Münzer, A. Neubauer, B. Pedersen, and A. Rosch, J. Phys.: Cond. Matt. **22**, 164207 (2010).
16. A. Neubauer, C. Pfleiderer, B. Binz, A. Rosch, R. Ritz, P. G. Niklowitz, and P. Böni, Phys. Rev. Lett. **102**, 186602 (2009).
17. W. Münzer, A. Neubauer, T. Adams, S. Mühlbauer, C. Franz, F. Jonietz, R. Georgii, P. Böni, B. Pedersen, M. Schmidt, A. Rosch, and C. Pfleiderer, Phys. Rev. B **81**, 041203 (2010).
18. H. Wilhelm, M. Baenitz, M. Schmidt, U.K. Rößler, A. A. Leonov, and A. N. Bogdanov, Phys. Rev. Lett. **107**, 127203 (2011).
19. E. Moskvin, S. Grigoriev, V. Dyadkin, H. Eckerlebe, M. Baenitz, M. Schmidt, and H. Wilhelm, Phys. Rev. Lett. **110**, 077207 (2013).
20. T. Adams, S. Mühlbauer, C. Pfleiderer, F. Jonietz, A. Bauer, A. Neubauer, R. Georgii, P. Böni, U. Keiderling, K. Everschor, M. Garst, and A. Rosch, Phys. Rev. Lett. **107**, 217206 (2011).
21. X. Z. Yu, Y. Onose, N. Kanazawa, J. H. Park, J. H. Han, Y. Matsui, N. Nagaosa, and Y. Tokura, Nature **465**, 901 (2010).
22. X. Z. Yu, N. Kanazawa, Y. Onose, K. Kimoto, W. Z. Zhang, S. Ishiwata, Y. Matsui, and Y. Tokura, Nat. Mater. **10**, 106 (2011).
23. A. Tonomura, X. Yu, K. Yanagisawa, T. Matsuda, Y. Onose, N. Kanazawa, H.S. Park, and Y. Tokura, Nano Lett. **12**, 1673 (2012).
24. U. K. Rößler, A. N. Bogdanov, and C. Pfleiderer, Nature **442**, 797 (2006).
25. U. R. Rößler, A. A. Leonov, and A. N. Bogdanov, J. Phys.: Conf. Ser. **303**, 012105 (2011).
26. A. Neubauer, C. Pfleiderer, B. Binz, A. Rosch, R. Ritz, P. G. Niklowitz, and P. Boni, Phys. Rev. Lett. **102**, 186602 (2009).
27. The internal magnetic field was calculated using the expression  $\mathbf{B}_{\text{int}} = \mathbf{B}_{\text{ext}} - 4\pi\mathbf{M}\hat{N}$ , where  $N$  was taken equal to 1 if  $\mathbf{H}$  is parallel to the normal of the sample plate. The magnetization was considered to be linear versus an external field  $M = \chi H$  with  $\chi = \text{const}$  depending on the temperature and extracted from the magnetization measurements. Thus corrected magnetic field may have a systematic error of order of 5 %.
28. N. Potapova, V. Dyadkin, E. Moskvin, H. Eckerlebe, D. Menzel, and S. Grigoriev, Phys. Rev. B **86**, 060406(R) (2012).
29. V. E. Dmitrienko and V. A. Chizhikov, Phys. Rev. Lett. **108**, 187203 (2012).
30. V. A. Chizhikov and V. E. Dmitrienko, Phys. Rev. B **88**, 214402 (2013).
31. O. Petrova and O. Tchernyshyov, Phys. Rev. B **84**, 214433 (2011).